Field dependence of the superconductive penetration depth in tin up to the superheating limit

Hugo Parr*
Institute of Physics, University of Oslo, Oslo 3, Norway
(Received 22 April 1975)

The superconductive penetration depth $\delta(T,H)$ has been studied as a function of temperature and field in single tin spheres, 15–30 μm in diameter. A mutual-inductance method was used with the 75-kHz measuring field parallel to the static field. When properly normalized, the variation of the transition signal with T and H is then proportional to $d[\bar{\delta}(T,H)\times H]/dH$, where $\bar{\delta}$ is the penetration depth averaged over the sphere surface. The results are independent of sphere diameter, and thus characteristic of bulk tin. In zero field, we find $\delta(T)=\delta_0/[1-(T/T_c)^4]^{1/2}$, with $\delta_0=520\pm30$ Å. The field dependence was studied for temperatures close to T_c and fields up to the ideal bulk superheating field $H_{sh}\cong 2.76H_c$, corresponding to a Ginzburg-Landau parameter $\kappa=0.093\pm0.001$. The penetration depth increases sharply as the field approaches H_{sh}, but stays finite, while its derivative diverges. We find $\delta(H_{sh})/\delta(H=0)=1.51\pm0.04$. Averaged over the sphere, we have $\bar{\delta}(H_{sh})/\bar{\delta}(H=0)=1.19\pm0.01$. The field dependence is rather well described by one-dimensional Ginzburg-Landau theory in the low-κ limit. The results indicate that the surface order parameter ψ_s is depressed by (30–50)% at H_{sh}. In "weak" fields, $H\leq 1.5H_c$, the data are consistent with the customary quadratic field dependence.

I. INTRODUCTION

The superconducting state is characterized by two fundamental microscopic lengths: the coherence length ξ and the penetration depth δ. The latter describes the decay of a static magnetic field from the surface of the superconductor towards its interior. Historically, the existence of the penetration depth was established in the 1930's, after the discovery of the Meissner effect in 1933.

The early studies[1-3] of the penetration depth in type-I superconductors established a very strong temperature dependence. Empirically, $\delta(T)$ is roughly proportional to $y=1/(1-t^4)^{1/2}$. Later and more precise experiments are still well described by this original experimental law, although there is a small deviation at low temperatures.[4-6] The field dependence of δ is much more elusive. Pippard[7] first established a small but definite field dependence in 1950. His experiments on tin gave an increase in δ on the order of (1–3)% as the field was increased from zero to H_c. Later experiments[8,9] have confirmed this small effect, giving a quadratic field dependence of the form $\delta\sim 1+\alpha H^2$, which is also predicted from Ginzburg-Landau (GL) theory in the weak-field limit.[10]

The present experiments extend the penetration-depth measurements into the metastable region above H_c. Ideal superheating, i.e., persistence of the superconductive state up to the field H_{sh} where homogeneous nucleation of the normal state occurs, was first observed by Feder *et al.* in experiments on In powders.[11] The powder method was subsequently used to investigate a number of materials. (See Refs. 12 and 13, and references therein). The experimental method was further refined by measurements on single, flawless spheres of diameters 5–30 μm.[14,15] This gives sharp, essentially widthless transitions, and moreover permits the determination of the penetration depth as well.[15] Single-sphere experiments have so far been carried out on Sn, In,[14] and β-Ga.[15] These experiments show that an ideal tin sphere will not go normal until the equatorial field reaches $H_{sh}=H_c/(\kappa\sqrt{2})^{1/2}=2.76\,H_c$, close to T_c. The single-sphere method offers a unique opportunity to study the metastable states above H_c which are usually inaccessible to observation because of nucleation by defects.

Information about the temperature and field dependence of the penetration depth is extracted from the variation of the transition signal between the superconducting and normal states. Two factors complicate the analysis. First, the spherical geometry gives a demagnetizing field, causing the total field to vary over the surface of the sphere. Any measurement of the penetration depth is thus an average over the spherical surface. Second, an ac tickling field *parallel* to the static field was used. This gives a much greater sensitivity than a perpendicular field, but it necessitates an integration over field to obtain the penetration depth. We shall show that these difficulties can be overcome, and that $\delta(T,H)$ can be extracted from the data. The results will show that $\delta(H)$ increases by about 50% to a finite value at H_{sh}, while its first field derivative diverges. Thus, the penetration depth of a type-I superconductor in "strong" fields has been measured for the first time.

II. THEORY

A. Penetration depth

For a 75-kHz measuring field, we have $\hbar\omega/\Delta(0) \simeq 5\times10^{-7}$. We need therefore only consider the static limit where no frequency corrections are necessary. The penetration depth for static magnetic fields is defined by

$$\delta \equiv \frac{1}{H(0)} \int_0^\infty H(x)\, dx , \tag{1}$$

where $H(0)$ is the field at the surface, and x is the distance from the surface of the superconductor. The definition is general; it does not assume any particular law of penetration. In particular, it gives the intuitive result for an exponentially decaying field, as obtained from the London equations. It is also correct for the nonphysical case, where H remains constant to a depth δ and then drops discontinuously to zero. We shall exploit this fact in making the approximations of Sec. II B.

The earliest estimate of the penetration depth is that of London, and is based on the free-electron model

$$\lambda_L(T) = [mc^2/4\pi e^2 n_s(T)]^{1/2} , \tag{2}$$

where n_s is the density of superconducting electrons in a two-fluid model. The values of $\lambda_L(0)$ for the elements are on the order of 100 Å, which is typically lower than the experimental values by a factor of 2 or 3. Pippard[16] was the first to explain why the observed penetration depth was larger than the London value. In type-I superconductors, $\lambda_L(0)$ is much smaller than the coherence length ξ_0, so that the local London equations must be replaced by nonlocal relations. The BCS theory gives a nonlocal relation equivalent to Pippard's. The BCS expression for the penetration depth in the limit $\lambda_L(0) \ll \xi_0$ is[17]

$$\delta_0 = [(\sqrt{3}/2\pi)\xi_0 \lambda_L^2(0)]^{1/3} , \tag{3}$$

$$\frac{\delta(T)}{\delta_0} = \left[\frac{\Delta(T)\tanh[\Delta(T)/2kT]}{\Delta(0)}\right]^{-1/3} . \tag{4}$$

A plot of the right-hand side of (4) against the empirical function $y = 1/(1-t^4)^{1/2}$ is virtually linear, except for $y<2$. The small deviation at low temperatures has been observed.[4,6] We shall see that the present experiments are very well described by $\delta(T) = \delta_0 y$, so we will not use the exact BCS expression.

The field dependence of δ is most easily treated by Ginzburg-Landau theory, where a depression of the surface order parameter ψ_s will lead to an increasing penetration depth as the field increases. Noticing that $n_s = \psi^2$, we have in the London limit, from Eq. (2), writing ψ for $|\psi|$,

$$\delta(H) \sim [\psi_s(H)/\psi_0]^{-1} . \tag{5}$$

In the nonlocal limit, from Eqs. (2) and (3),

$$\delta(H) \sim [\psi_s(H)/\psi_0]^{-2/3} , \tag{6}$$

where ψ_0 is the (constant) order parameter in the interior of the superconductor. For weak fields and $\kappa \ll 1$, the original GL theory[10] gave

$$\psi_s/\psi_0 \cong 1 - (\kappa/4\sqrt{2})(H/H_c)^2 . \tag{7}$$

Combining Eqs. (5)-(7), we obtain

$$\delta(H)/\delta(0) \cong 1 + (\kappa/4\sqrt{2})(H/H_c)^2 \quad \text{(weak field, local theory)}, \tag{8}$$

$$\delta(H)/\delta(0) \cong 1 + (\kappa/6\sqrt{2})(H/H_c)^2 \quad \text{(weak field, nonlocal theory)}, \tag{9}$$

Thus, in both cases, $\delta(H) \sim 1 + \alpha(H/H_c)^2$. For tin, $\kappa = 0.093$ (Sec. IV C). This gives $\alpha = 0.016$ and 0.011 for the local and nonlocal cases, respectively.

A perfect sample can be kept superconducting in fields much larger than H_c. The limiting field for the metastable, superheated state for $\kappa \ll 1$ is given by[18,19]

$$H_{sh} = H_c/(\kappa\sqrt{2})^{1/2} . \tag{10}$$

This is the field at which homogeneous nucleation of the normal state occurs. For tin, this gives $H_{sh} = 2.76 H_c$ at $t = 1$. In "strong" fields approaching H_{sh}, the weak-field approximation used to derive Eq. (7) is no longer valid. A one-dimensional calculation was made for $\kappa \ll 1$ (see Ref. 19), and the GL equations were solved for all fields. The result is

$$[\psi_s(H)/\psi_0]^2 = \tfrac{1}{2}\{1 + [1 - (H/H_{sh})^2]^{1/2}\} . \tag{11}$$

For weak fields $H/H_{sh} \ll 1$, this reduces to Eq. (7), as it should. Close to H_{sh}, the ratio ψ_s/ψ_0 approaches the finite value $1/\sqrt{2}$, while the derivative $d\psi_s/dH$ diverges. This last prediction is, in fact, typical for any mean-field theory giving an expression for $\psi(H)$ as the field increases towards the limit of metastability. At this limit, the two curves in the ψ-H plane which describe a local minimum and a local maximum of the free energy F, join in a single point which is an inflexion point in the F-ψ plane. Therefore, one would expect $dH/d\psi = 0$ at this point. The present experiments will provide the first observational test.

Combining Eq. (11) with Eqs. (5) and (6), GL theory predicts

$$\delta(H_{sh})/\delta(0) = \begin{cases} 1.41 & \text{(local case)}, \\ 1.26 & \text{(nonlocal case)}. \end{cases}$$

Furthermore, the derivative of δ at H_{sh} should di-

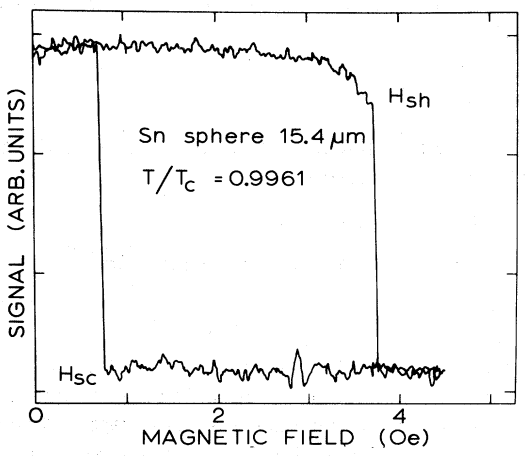

FIG. 1. Recorder trace of field sweep for a 15.4-μm-diam tin sphere, with the ac measuring field parallel to the static field. In the superconducting state (top) the signal shows a marked depression close to the superheating field H_{sh}, whereas in the normal state the signal is constant (bottom). Signal depression is caused by the increase with field of the superconductive penetration depth δ.

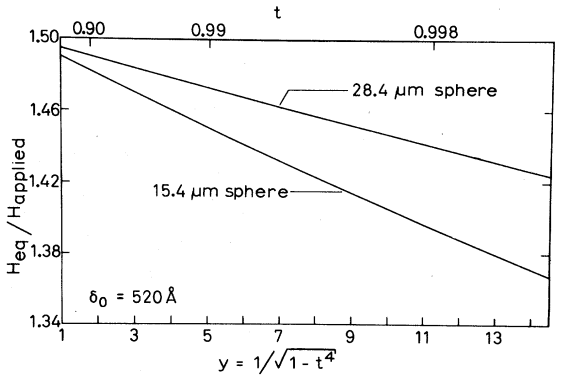

FIG. 2. Demagnetization coefficient $k(T) = H_{\text{equatorial}}/H_{\text{applied}}$ for two tin spheres [Eq. (16)]. Increasing penetration depth causes $k(T)$ to decrease with temperature. For a large sphere, $k = \frac{3}{2}$.

verge in both cases. A weak-field expansion gives

$$\delta(H)/\delta(0) = 1 + \tfrac{1}{8}(H/H_{sh})^2 + \tfrac{7}{128}(H/H_{sh})^4 \cdots \quad \text{(local case)}, \quad (12)$$

$$\delta(H)/\delta(0) = 1 + \tfrac{1}{12}(H/H_{sh})^2 + \tfrac{5}{144}(H/H_{sh})^4 \cdots \quad \text{(nonlocal case)}. \quad (13)$$

Expressing H_{sh} in terms of H_c and κ, the quadratic terms in Eqs. (12) and (13) reduce to those of Eqs. (8) and (9).

B. Variation of signal with temperature and field

1. V_{eff} approximation

Let S be the observed *difference* in mutual-inductance signal between the superconducting and normal states. As the penetration depth varies with temperature and field, the effective superconductive volume of the sample will vary, and hence S will vary. Figure 1 shows an experimental hysteresis loop for a 15.4-μm-diam tin sphere close to T_c. S is seen to decrease markedly close to the superheating transition. This decrease is caused by an increase of the penetration depth with the field. The transition itself is sharp, irreversible, and always reproducible, ruling out the possibility that the decrease in signal preceding it could be due to dissipative effects. Indeed, any normal domain would immediately nucleate the full transition to the normal state. A study of the 3rd harmonic signal further supports this conclusion. When a sphere is in the intermediate state, the 3rd harmonic signal has been observed to be strong and irregular. For the tin spheres presently investigated, the 3rd harmonic signal was small, giving a clean hysteresis loop similar to that of Fig. 1 except for a higher noise level. Thus, the sphere is in the Meissner state all the way up to the superheating transition.

The question is how to relate changes in signal S to changes in the penetration depth. Changes with temperature at $H=0$ are simple to analyze, but the analysis of the field dependence is nontrivial, and has not been carried out before. It is made complicated by two factors: (a) the use of an ac measuring field parallel to the static field; (b) the spherical geometry which makes the surface field vary with the polar angle. Any measurement of the penetration depth is thus an average over the surface.

We first observe that even very close to T_c, the sphere radius R is much bigger than $\delta(T,H)$. In fact, at $t=0.998$, $\delta(T)/R \cong 0.07$ for the smallest sphere. We can therefore define an effective superconductive volume V_{eff} as follows: At a point on the surface with polar angle θ, there is a local field H_θ and a local penetration depth $\delta(T,H_\theta)$. Imagine this penetration depth shaved off the sphere, giving an ellipsoidal body flattened at the equator. This body can be treated as perfectly diamagnetic, with a volume

$$V_{\text{eff}}(T,H) = \tfrac{4}{3}\pi \int_0^{\pi/2} d\theta \sin\theta [R - \delta(T,H_\theta)]^3 . \quad (14)$$

This simplification is justified by Eq. (1) and by the fact that δ/R is so small that the surface is "flat" on the scale of δ. The field distribution H_θ is not known for the general case of a field-dependent penetration depth. However, for a constant penetration depth, the boundary-value

problem was solved by London,[20] giving to second order in δ/R

$$H_\theta = H_{eq} \sin\theta = k(T) H \sin\theta , \tag{15}$$

$$k(T) = \tfrac{3}{2}[1 - (\delta_0 y/R) + (\delta_0 y/R)^2] . \tag{16}$$

Here, H is the applied field, and we have assumed $\delta(T) = \delta_0 y$, where $y = 1(1 - t^4)^{1/2}$. This assumption will be justified by the experimental results. Figure 2 shows the ratio $k(T) = H_{eq}/H$ for two of the spheres investigated as a function of y. Since the penetration depth increases with H, Eqs. (15) and (16) are only valid as $H \to 0$. For any finite H, the field penetrates further at the equator than at the poles, giving a ratio H_{eq}/H slightly *less* than $k(T)$. However, we will show that only a small error is induced by using Eqs. (15) and (16) for all fields. We anticipate from the experimental results that δ increases by about 50% from $H = 0$ up to the superheating limit. For fields approaching H_{sh}, a more realistic angular field distribution than Eq. (15) would be

$$H_\theta \simeq [k(T)\cos^2\theta + k'(T)\sin^2\theta] H \sin\theta ,$$

where $k'(T)$ is obtained from Eq. (16) using the equatorial penetration depth $\delta(T, H_{sh}) \simeq 1.5\delta_0 y$. This modified field distribution in fact probably overestimates the correction due to the field dependence. Anticipating Eq. (26), the measured quantity will be the penetration depth averaged over the sphere surface:

$$\frac{\bar{\delta}(H)}{\delta(H=0)} = \int_0^{\pi/2} d\theta \sin\theta f\left(\frac{H_\theta}{H_{eq}}\right),$$

where f is the field dependence we seek. Using the GL expression, with $f \sim 1/\psi_s$ from Eq. (11), we obtain for the 15.4-μm sphere at $t = 0.99$ an averaged penetration depth $\bar{\delta}(H_{sh})/\delta(0) = 1.171$ using Eq. (15), and 1.179 using the improved field distribution. The difference is less than what the experimental error will turn out to be (Sec. IV B). We are therefore justified in using the London field distribution for all fields. Equation (14) then simplifies to

$$V_{eff}(T, H) = \tfrac{4}{3}\pi R \int_0^{\pi/2} d\theta \sin\theta (R^2 - 3R\delta + 3\delta^2) ,$$

$$\delta = \delta(T, k(T) H \sin\theta) . \tag{17}$$

Here, we have included terms up to δ^2.

The signal measures the derivative of the magnetization $M \sim H V_{eff}$. Thus

$$S(T, H) \sim \frac{d}{dH}[H V_{eff}(T, H)] . \tag{18}$$

Here, we assume the amplitude of the measuring field to be negligible compared to the static field. If the measuring field is perpendicular to the static field,

$$\frac{dV_{eff}}{dH} = 0$$

to first order, because the scalar value of the total field does not change. Thus

$$S_\perp(T, H) \sim V_{eff}(T, H) , \tag{19}$$

whereas for a parallel measuring field

$$S_\parallel(T, H) \sim V_{eff}(T, H) + H \frac{dV_{eff}}{dH} . \tag{20}$$

As we shall see, the second term in Eq. (20) dominates, and makes it advantageous to use parallel fields to increase the sensitivity. Thus, in Fig. 1, the signal depression close to H_{sh} for perpendicular fields would have been only about $\frac{1}{10}$ of that shown, making the field effect almost undetectable. This explains why no field effect was seen in our previous experiments on β-Ga,[15] where perpendicular fields were used.

2. *Temperature dependence*

For $H = 0$, $S \sim V_{eff}$ in both of the above cases, and the analysis is straightforward. Assuming again $\delta(T) = \delta_0 y$, we get from Eq. (17)

$$\frac{S(T, 0)}{S(0, 0)} = \frac{1 - 3\delta_0 y/R + 3(\delta_0 y/R)^2}{1 - 3\delta_0/R + 3(\delta_0/R)^2} . \tag{21}$$

Fitting this equation to the experimental results gives $S(0, 0)$ and δ_0. In practice, we use the signal at the supercooling transition where the field effect is negligible, so that $S(T, H_{sc}) \cong S(T, 0)$.

3. *Field dependence*

To extract the field dependence, it is necessary to normalize away the temperature dependence of the signal. Let

$$\delta(T, H) \equiv \delta(T, 0) f(H/H_c) , \tag{22}$$

where f is the unknown function to be determined by experiment. Define a reduced signal

$$\zeta \equiv [S^0 - S(T, H)]/[S^0 - S(T, 0)] , \tag{23}$$

where

$$S^0 \equiv S(0, 0)/[1 - 3\delta_0/R + 3(\delta_0/R)^2] . \tag{24}$$

S^0 is the hypothetical signal for the case of zero penetration depth and is determined experimentally by extrapolating Eq. (21) to $y = 0$. Next, define a reduced field

$$h \equiv H_{eq}/H_c = k(T) H/H_c(T) . \tag{25}$$

Substituting from Eqs. (17) and (19) into Eq. (23), we get for perpendicular fields, and to first order

in δ/R,

$$\zeta_\perp(h) \cong \int_0^{\pi/2} d\theta \sin\theta f(h\sin\theta)$$

$$\equiv \bar{f}(h) \equiv \bar{\delta}(h)/\delta(h=0). \tag{26}$$

Notice that, to first order, the reduced signal $\zeta_\perp$ is a function of h alone, not of T. In fact, $\zeta_\perp$ is seen to be an average over the spherical surface of the function f, with a weight factor $\sin\theta$ which makes the region around the equator contribute most to the integral. We shall denote this average by $\bar{f}$ or by $\bar{\delta}(h)/\delta(0)$. To second order, we find

$$\zeta_\perp \cong \int d\theta \sin\theta f(h\sin\theta)\left(1 - \frac{\delta(T,0)}{R}\left[f(h\sin\theta) - 1\right]\right). \tag{27}$$

To an excellent approximation, f in the right-hand factor can be replaced by $\bar{f}$ and brought outside the integral. This gives a self-consistent equation which can be solved with respect to $\bar{f}$, yielding

$$\bar{f} = \zeta_\perp\left(1 + \frac{\delta(T,0)}{R}(\zeta_\perp - 1)\right). \tag{28}$$

Compared with the first-order expression, Eq. (26), the second-order correction gives values for $(\bar{f}-1)$ which are (3–4)% higher for a 15-μm-diam sphere at $t \cong 0.99$.

Turning to the case of parallel fields, Eqs. (17), (20), and (23) yield, to first order,

$$\zeta_\parallel(h) \cong \frac{d}{dh}\left(h\int_0^{\pi/2} d\theta \sin\theta f(h\sin\theta)\right). \tag{29}$$

To second order, we get

$$\zeta_\parallel = \frac{d}{dh}\left[h\int_0^{\pi/2} d\theta \sin\theta f \times \left(1 - \frac{\delta(T,0)}{R}(f-1)\right)\right]. \tag{30}$$

We define a new function $Z(h)$:

$$Z(h) \equiv \frac{1}{h}\int_0^h \zeta_\parallel(h')\,dh'. \tag{31}$$

After integrating Eq. (30) with respect to the field, we again get a self-consistent equation for $\bar{f}$, leading to

$$\bar{f}(h) = Z\left(1 + \frac{\delta(T,0)}{R}(Z-1)\right). \tag{32}$$

Notice that $\bar{f} = Z$ to first order.

We have now laid the foundations for analyzing the data. For the parallel-fields case, this analysis proceeds as follows. From the data $S(T,H)$, we calculate the reduced signal $\zeta_\parallel$, Eq. (23). To first order, this is only a function of the reduced field $h = H_{eq}/H_c$. The integration over the field, Eq. (31), can be carried out model independently by joining all the experimental points $\zeta_\parallel(h)$ by a zigzag line, and integrating under this curve from 0 to h, thus obtaining $Z(h)$. From $Z(h)$, $\bar{f}(h)$ is calculated correctly to second order in δ/R, using Eq. (32). The final step consists in determining the unknown function $f(h)$ from $\bar{f}(h)$, using the defining Eq. (26). We have not succeeded in inverting this integral analytically, so at this point $f(h)$ must be determined either by trial and error, or by expressing $\bar{f}(h)$ as a sum whose terms can be individually inverted, for instance as a power series.

The above concepts can be illustrated by assuming $f = 1 + \alpha(H/H_c)^N$. With $h = H_{eq}/H_c \simeq \frac{3}{2}H_c$, this gives

$$\zeta_\perp(h) = Z(h) = 1 + j_{N+1}\alpha h^N,$$
$$\zeta_\parallel(h) = 1 + (N+1)j_{N+1}\alpha h^N, \tag{33}$$

where

$$j_N \equiv \int_0^{\pi/2} \sin^N\theta\, d\theta. \tag{34}$$

We see that the field effect for parallel fields is $(N+1)$ times enhanced. In particular, for $N=2$, the observed effect in parallel fields is enhanced by a factor of 3, as pointed out in the original Ginzburg-Landau paper.[10] If the field dependence could be described by such a simple power law, there would be no need for the elaborate machinery of Eqs. (26)–(32). However, we shall see that f has a singularity at H_{sh}, so that a general analysis is necessary.

III. EXPERIMENTAL

The tin[21] spheres were produced by sonoration of the molten metal in pure 1-2-6 hexanetriol, and repeatedly rinsed in pure alcohol. Single spheres were selected under the microscope. Sphere diameters were measured in the microscope to an accuracy of ± 0.5 μm.

The cryostat and detection system have been described before.[15,22] A germanium thermometer calibrated against ^{4}He vapor pressure was used. Temperatures could be stabilized to about 0.1–0.2 mK. T_c was determined for each sphere from a zero-field sweep of the type shown in Fig. 2 of Ref. 22. This gives T_c with a relative accuracy of ± 0.2 mK. Field sweeps at temperatures close to T_c were reversed so as to eliminate small axial remanent fields. The effect of the tickling field was corrected for by doing sweeps for different tickling fields, and extrapolating to zero. The 75-kHz tickling field was typically 0.2–0.6 Oe

peak to peak and parallel to the static field. Some experimental parameters for the three spheres investigated are given in Table I.

It was necessary to measure the signal difference S between the superconducting and normal state as accurately as possible (see Fig. 1). Measuring S directly from the hysteresis loop is not good enough since the signal will often drift with time. The following procedure was therefore used. The field sweep was stopped at the desired value of H, and a 100-msec current transient was applied to the solenoid, causing a transition in the sphere. After 10 sec, when all electrical and thermal transients had died out, the signal difference was measured. To improve accuracy, each transition was repeated 5 or 10 times. This permitted measurement of $S(T,H)$ to respective accuracies of about 2 and 1% for the 15.4- and 28.4-μm spheres. Measurements were performed for $H_{sc} \leq H \leq H_{sh}$.

A problem was encountered in that the total output signal, of which the transition signal is only a small part, was found to decrease slowly with time on the average by 10% in 4 h. This is probably due to the sinking He level, which changes the resonance conditions in the detection system. However, it was established that the transition signal was always proportional to the total signal. The total signal was therefore monitored, and the transition signal corrected proportionally.

IV. RESULTS

Experiments were performed on the three tin spheres of Table I. The main series of measurements was carried out on the 15.4-μm sphere. A few measurements on a 17.1-μm sphere confirmed that the results on the first sphere were reproducible. Both these spheres showed ideal superheating and supercooling. Finally, to see if the field effect depended upon the size of the sphere, a series of experiments was carried out on a 28.4-μm sphere. Unfortunately, this sphere had some surface defects, and only superheated to about $2.5H_c$. The results below this field, however, are in accordance with those on the smaller spheres, and show the field dependence to be a bulk effect. In the following, we first report the results on the penetration depth $\delta(T,H)$ and then give the results on the superheating and supercooling.

TABLE I. Experimental parameters for three tin spheres.

Sphere	Diameter (μm)	T_c (K)	Peak-to-peak tickling field (Oe)
Sn-1	15.4	3.7239	0.48
Sn-2	17.1	3.7195	0.62
Sn-3	28.4	3.7231	0.28

A. Penetration depth: temperature dependence

At H_{sc}, the equatorial field is less than $0.4\,H_c$, so any field effect is negligible. We therefore use the temperature variation of the supercooling transition signal $S(T,H_{sc})$ to determine $\delta(T)$. Assuming $\delta(T)=\delta_0 y$, where $y=1/(1-t^4)^{1/2}$, we can fit the experimental data to Eq. (21) to determine δ_0. The results for the 15.4- and 28.4-μm spheres are shown in Fig. 3. We see that the signal depression from $t=0$ to $t=0.998$ is about 19 and 11%, respectively. At least-mean-squares fit gives $\delta_0=500\pm40$ Å for the smaller sphere and $\delta_0=530\pm30$ Å for the bigger one. The best experimental value is thus

$$\delta_0=520\pm30\ \text{Å}.$$

The theoretical curves in Fig. 3 are calculated from this value, and are seen to fit the experimental points very well. The agreement with previous experiments is excellent: our value of δ_0 is identical with that obtained by Laurmann and

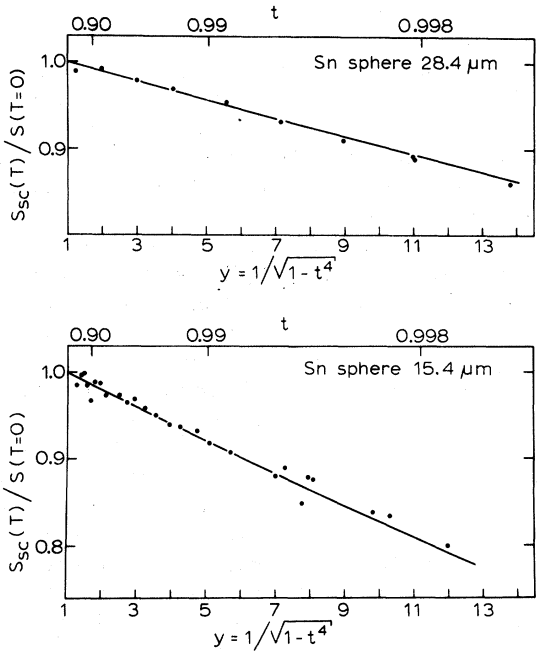

FIG. 3. Temperature dependence of the signal, reflecting the temperature dependence of the penetration depth δ. Solid curves correspond to $\delta(T)=\delta_0/(1-t^4)^{1/2}$, with $\delta_0=520$ Å. Signal is seen to decrease by about 20% for the smaller sphere from $t=0$ to $t=0.998$.

Shoenberg[3] and with the value obtained by Schawlow and Devlin[4] above $y=1.7$. However, it must be emphasized that this is no *absolute* determination of the penetration depth at $T=0$. Instead, we have measured *changes* in δ with temperature and found that these can be described by $\delta(T)=\delta_0 y$. An absolute determination of $\delta(T=0)$ is impossible from this kind of experiment, as pointed out by Tedrow *et al.*[23]

B. Penetration depth: field dependence

In the following, we will extract the field dependence $f(H/H_c)$ of the penetration depth from the experimental data $S(T,H)$ proceeding as outlined in Sec. II B 3. While data were collected down to $t=0.6$, we will use only the data close to T_c in this analysis. The main reason is that the changes in signal are proportional to the product $\delta(T)f(h)$, and thus the experimental resolution of the field effect is proportional to $y=1/(1-t^4)^{1/2}$. Hence, going from $t=0.996$ ($y\simeq 8$) to $t=0.88$ ($y\simeq 1.6$) decreases the experimental sensitivity by a factor of 5. Also, the superheating may not be ideal far from T_c. On the other hand, if field sweeps are taken too close to T_c, the temperature stability becomes critical, and the tickling field can no longer be neglected compared with the static field. We therefore choose for analysis the data for which $0.965<t<0.996$. This still corresponds to a large spread in the values of y, which range from 2.7 to 7.9.

Figure 4 shows the reduced signal $\zeta_{\parallel}$ for the 15.4- and 28.4-μm spheres. Each data point is the average of 5 or 10 transitions, as explained in Sec. III. Thus, the 74 points shown for the smaller sphere represent a total of 460 individual transitions. ζ is plotted as a function of the reduced field $h=H_{eq}/H_c$. H_c is taken from the literature (see Sec. IV C), and $H_{eq}=k(T)H$, where H is the applied field and $k(T)$ is the demagnetizing coefficient given by Eq. (16) and plotted in Fig. 2. The asymptotic value $H_{sh}^{bulk}/H_c=2.76$ is determined from the GL parameter $\kappa(t=1)=0.093$ (Sec. IV C). Since κ changes slightly with temperature even in the small temperature range represented in Fig. 4, all values of h have been scaled to give $H_{sh}^{bulk}=2.76\,H_c$, which is strictly true only at $t=1$. Otherwise we would have a "fuzzy" asymptote which would move to slightly lower values of h for the data with lower t because of the increase in κ. As Fig. 4 now stands, it is *characteristic of bulk tin at $t=1$*. The same is true for all subsequent figures.

As explained in Sec. II B 3, the reduced signal ζ should be a function of h alone, to first order in δ/R. Figure 4 contains data for different temperatures, which indeed fall on a universal curve within the experimental accuracy. These results are unchanged by halving the tickling field. For the smaller sphere, we see that ζ increases from its initial value of 1 at $h=0$ to values approaching 3 close to the bulk superheating field. The increase is scarcely noticeable below $h=1$, but becomes very strong close to $h_{sh}=2.76$. The reproducibility of the data for the 15.4-μm sphere was established by experiments on two other spheres. The few measurements on the 17.1-μm sphere (not shown) gave values for ζ of 2–2.8 in the vicinity of the superheating transition, in agreement with Fig. 4. The results for the bigger sphere, 28.4 μm in diameter, are given in the upper part of Fig. 4. Unfortunately, this sphere had surface defects preventing ideal superheating. However, as seen from the figure, this sphere gives values of ζ around 1.6 at $h=2.5$, in very good agreement with the data for the smaller sphere at that same reduced field. We can thus draw the conclusion that the field effect is reproducible and independent of sphere diameter, i.e., characteristic of bulk tin.

The results presented in Fig. 4 lead to an important conclusion which is not readily apparent. Namely, the field effect is governed by the *bulk* superheating field H_{sh}^{bulk} and not by the *actual* superheating field H_{sh}. For an ideal sphere, these fields are identical for temperatures up to about $t=0.985$ for a diameter of 15.4 μm. At this point, even in an ideal sphere, a size effect in the coherence length sets in which reduces the width of the observed field hysteresis and makes the parameters κ_{sc} and κ_{sh} apparently diverge. This effect is well known from earlier experiments[14,15] and is observed in the present experiments as well. (See the superheating/supercooling results, presented in Sec. IV C and Fig. 9.) However, the results for $\zeta(h)$ do not seem to be influenced by this size effect in the coherence length. For instance, the superheating transition at $t=0.982$ occurs at $h=2.72$, very close to the bulk value of 2.76, and gives $\zeta=2.62$. At $t=0.996$, well into the size-effect region, the observed superheating transition occurs at $h=2.58$, giving $\zeta=1.77$, which falls very nicely on the universal curve of Fig. 4. We conclude that the field effect is governed by H_{sh}^{bulk}, even as the observed $H_{sh}<H_{sh}^{bulk}$, because of the size effect in the coherence length.

In the subsequent analysis, we will use the data for the 15.4-μm sphere only, as they are the most complete, and extend to the ideal superheating field. Figure 5 shows the results for the mean penetration depth $\bar{\delta}(h)$ averaged over the surface of the sphere [Eq. (26)]. The points in Fig. 5 were obtained by connecting all the data points in the lower part of Fig. 4 by one continuous zigzag line and then integrating under this curve with

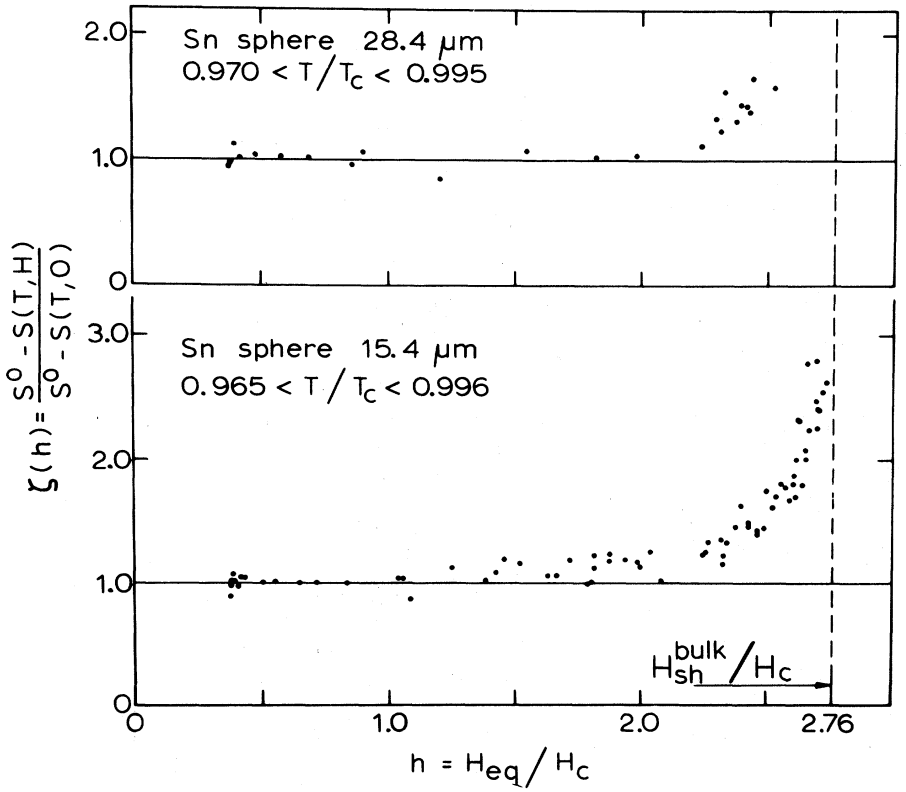

FIG. 4. Reduced signal $\zeta(h)$ for two tin spheres. To first order in δ/R, ζ is a function only of the reduced field $h = H_{eq}/H_c$. Data points shown are taken at different temperatures, but fall on a universal curve showing a sharp increase close to the superheating limit.

respect to h. This in turn yields $Z(h)$ [Eq. (31)] and $\bar{f}(h) \equiv \bar{\delta}(h)/\delta(h=0)$ [Eq. (32)]. The data of Fig. 5 were adjusted to give $\bar{\delta}(h)/\delta(0) = 1$ at $h = 0$ by means of a least-mean-squares fit of $\bar{\delta}$ vs h^2 for $h < 1.9$, correcting for the term in h^4 [Eqs. (12) and (26)]. It is apparent from Fig. 5 that the integration over field has greatly reduced the experimental scatter, especially at high fields $h > 2.3$,

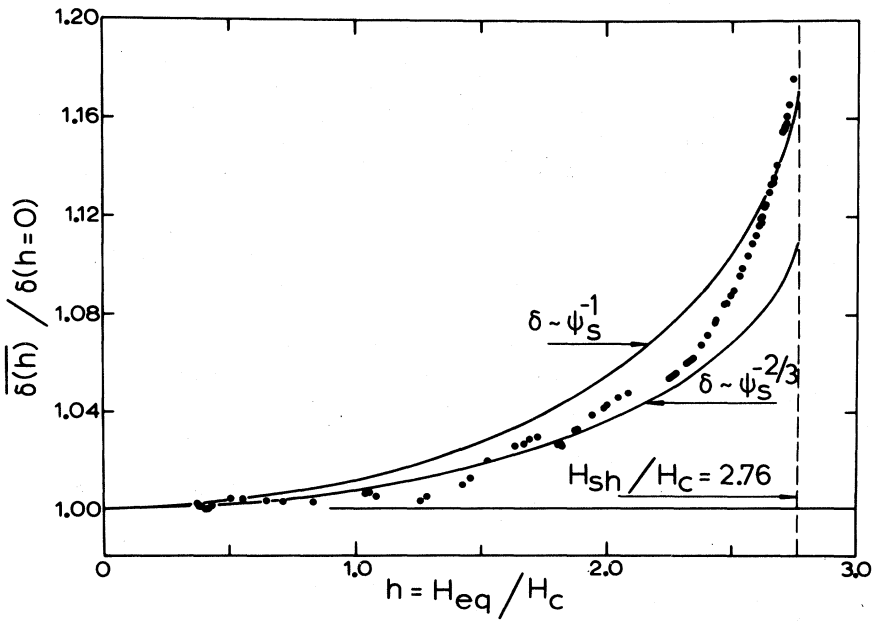

FIG. 5. Average value $\bar{\delta}$ over the spherical surface of the penetration depth. Extrapolation gives $\bar{\delta}/\delta(0) = 1.19$ at the superheating limit. Figure was obtained by graphical integration of Fig. 4, as explained in the text.

where the sensitivity is largest. However, the field effect itself is now seen to be quite small, at least when averaged over the spherical surface. The two solid curves in Fig. 5 give $\bar{\delta}(h)$ as predicted from the one-dimensional GL theory [Eq. (11)] for the local and nonlocal cases. They were calculated by numerical integration of Eq. (26), with $f(h)$ given by Eqs. (5), (6), and (11). They are in fair, but not complete, agreement with the experiments. The "nonlocal" curve, given by $\delta \sim \psi_s^{-2/3}$, gives the best description at low fields, whereas at high fields the experimental curve increases faster than either of the theoretical predictions. Thus, at the superheating field, $\bar{\delta}_{\rm exp}$ lies slightly above even the "local" curve given by $\delta \sim \psi_s^{-1}$.

The final step in the analysis is to invert the integral expression for $\bar{f}(h)$, Eq. (26), so as to obtain the unknown function $f(h) \equiv \delta(h)/\delta(h=0)$ from the averaged quantities. We are unable to do this analytically, and therefore proceed empirically by defining a deviation function $D(h)$ such that

$$\delta_{\rm exp}(h)/\delta(h=0) = f(h) \equiv (\psi_s/\psi_0)^{-1} - D(h) . \tag{35}$$

Here, ψ_s is the GL expression [Eq. (11)]. When averaged over the sphere by Eq. (26) this gives

$$\bar{f}_{\rm exp}(h) = \langle (\psi_s/\psi_0)^{-1} \rangle_{\rm av} - \bar{D}(h) . \tag{36}$$

The first term can be calculated numerically, and is given by the upper solid curve in Fig. 5. $\bar{D}(h)$ is determined empirically as the difference between this curve and the experimental points. We notice that this difference is zero at $h=0$ and $h=2.66$, with a maximum around $h=2.3$. We therefore try a deviation function of the form

$$\bar{D}(h) = 0.0058 h^2 [1 - (h/2.66)^8] . \tag{37}$$

The numerical coefficient comes from the least-mean-squares fit of $\bar{f}$ vs h^2 for low fields. The exponent 8 is chosen so as to make $\bar{D}$ a maximum close to $h=2.3$. The resulting function describes the experimental data of Fig. 5 quite well, smoothing out the "noise" at low h, and following the points for $h<2.3$ very accurately. It can also be written

$$\bar{D}(h) = 0.04418 (h/h_{\rm sh})^2 - 0.05936 (h/h_{\rm sh})^{10} , \tag{38}$$

where $h_{\rm sh} = 2.76$. We notice that the two theoretical curves in Fig. 5 give finite values of $\bar{f}$ of 1.171 and 1.110, respectively, at the superheating field. The experimental value is obtained by extrapolating Eqs. (36) and (38):

$$\bar{\delta}(h_{\rm sh})/\delta(h=0) = 1.19 \pm 0.01 .$$

Using Eq. (26), $D(h)$ is readily calculated, yielding

$$D(h) = (0.04418/J_3)(H/H_{\rm sh})^2 - (0.05936/J_{11})(H/H_{\rm sh})^{10} .$$

Here, $J_3 = \frac{2}{3}$ and $J_{11} = 0.3694$ are obtained from Eq. (34). The end result is

$$\delta_{\rm exp}(H)/\delta(H=0) = (\psi_s/\psi_0)^{-1} - 0.0663 (H/H_{\rm sh})^2 + 0.1607 (H/H_{\rm sh})^{10} , \tag{39}$$

where $H_{\rm sh} = H_c(\kappa\sqrt{2})^{1/2} = 2.76 H_c$, and $\psi_s(H/H_{\rm sh})$ is the GL expression [Eq. (11)]. We emphasize that Eq. (39) is a purely empirical fit to the data. Strictly speaking, it is only valid up to the last experimental point at $h=2.74$, and not all the way to the superheating limit. However, the experimental curve is so similar to the theoretical curves (Fig. 5) that we permit extrapolation to the superheating field, $2.76 H_c$. In Fig. 6, we have plotted the experimental curve for $f(H/H_c)$, together with the prediction $f = \psi_s^{-1}$. We believe that the uncertainty introduced by the approximations made, by the choice of an asymptote, by the tickling field and by the experimental scatter, amounts to no more than 8% in $(f-1)$ at the superheating limit. Thus, using Eq. (39), we have

$$\delta(H_{\rm sh})/\delta(H=0) = 1.51 \pm 0.04 .$$

The use of a more realistic angular field distribution H_θ (Sec. II B 1) would reduce the above value by an amount at most equal to the error given. Our value is slightly higher than $[\psi_s(H_{\rm sh})/\psi_0]^{-1} = 1.41$, but considerably higher than $(\psi_s/\psi_0)^{-2/3} = 1.26$. In the weak-field limit, Eq. (39) reduces to

$$\delta(H)/\delta(0) = 1 + \alpha (H/H_c)^2 ,$$

where $\alpha = 0.008 \pm 0.004$ from the least-mean-squares fit. This is less than the value of 0.0165 and 0.011 predicted by GL theory for the local and nonlocal cases, Eq. (8) and (9). Experimentally, Sharvin and Gantmakher[8] found α in the range 0.014–0.020 for tin, with the lower limit as the most reliable. However, the "noise" in the experimental points for low h in Fig. 5 show that the error in our value of α may be greater than given by the fit. Thus, our rather inaccurate value of α is in reasonable agreement with GL predictions and the previous experiment.

Since theory predicts that the derivative $f'(h)$ diverges at the superheating field (Sec. II), it is of interest to look more closely at this derivative. Figure 7 shows the experimental results for $\bar{f}'(h)$, the derivative averaged over the sphere. It is defined by

$$\bar{f}'(h) = \int_0^{\pi/2} d\theta \sin^2\theta f'(h \sin\theta) . \tag{40}$$

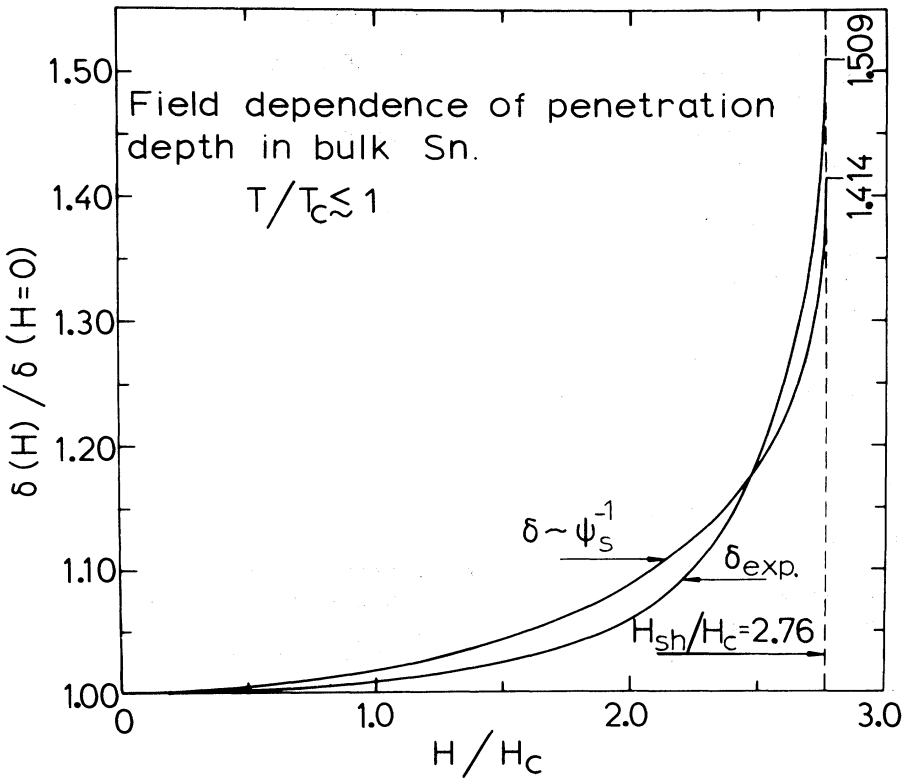

FIG. 6. Final results for the field dependence of the penetration depth at $t \approx 1$ in tin. Experimental curve was obtained from Fig. 5 by empirically inverting Eq. (26). Theoretical curve is based on $\psi_s(H)$ as given by the GL calculation, Eq. (11).

As seen from Eq. (29), it is obtained to first order in δ/R simply by subtracting the data points of Fig. 5 from those of Fig. 4, and then dividing by h:

$$\bar{f}' = (1/h)(\zeta - \bar{f}) . \tag{41}$$

Figure 7 shows that $\bar{f}'(h)$ is sharply increasing close to the superheating limit, where it lies consistently above the values given by $f \sim \psi_s^{-1}$, which itself has a divergent derivative $f'(h)$. Hence, in all probability $f'(H)$ diverges at H_{sh}, although this of course cannot be proven rigorously.

Finally, in Fig. 8, we present results on the field effect for temperatures down to $t = 0.78$. As the sensitivity drops rapidly with a lower t, we only present the reduced signal ζ at the superheating transition. We are not including data above $t = 0.98$, because of the size effect in H_{sh}, as explained earlier. Figure 8 shows that the reduced signal at H_{sh} decreases slowly as the tem-

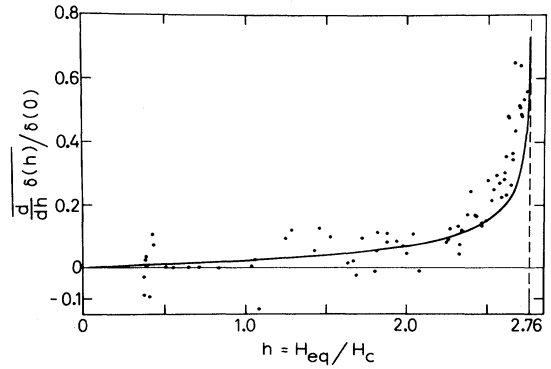

FIG. 7. Average over surface of the derivative of the penetration depth. Experimental points indicate a divergence at the superheating limit. Solid curve is based on $f \sim \psi_s^{-1}$.

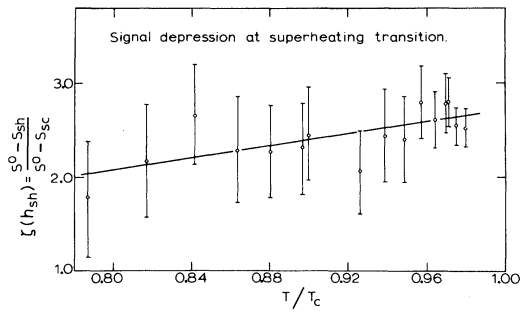

FIG. 8. Reduced signal at the superheating transition, as a function of temperature down to $t = 0.78$. Temperature dependence is seen to be slight.

perature is lowered. However, the uncertainty in the slope is seen to be considerable, and part of the decrease could be caused by deviations from ideality at the lower temperatures. We conclude that the field effect shows no marked change with temperature down to $t = 0.78$. In particular, we see no signs of the marked structure at $t = 0.80$–0.85 reported in Pippard's early work.[7]

C. Superheating and supercooling

The superheating and supercooling results are analyzed as usual[14,15] in terms of the experimental parameters

$$\kappa_{sc} = 0.4172(H_{sc}/H_c)\,, \tag{42}$$

$$\kappa_{sh} = \tfrac{1}{2}\sqrt{2}(H_c/\tfrac{3}{2}H_{sh})^2 = 0.3143(H_c/H_{sh})^2\,, \tag{43}$$

$$\kappa_{sh}^{\bar\delta} = \tfrac{1}{2}\sqrt{2}\{H_c/[k(T)H_{sh}]\}^2\,, \tag{44}$$

$$\kappa_R^{\bar\delta} = 0.4974\{H_{sc}/[k(T)H_{sh}]\}^{2/3}\,. \tag{45}$$

Here, H_{sh} and H_{sc} are the observed fields. Equation (43) assumes a spherical demagnetization coefficient of $\frac{3}{2}$, as for a large sphere. Equations (44) and (45) use the correct coefficient $k(T, H_{sh}) < \frac{3}{2}$, where

$$k(T, H_{sh}) = \tfrac{3}{2}[1 - \bar\delta/R + (\bar\delta/R)^2]\,, \tag{46}$$

$$\bar\delta(T, H_{sh}) = 1.19\delta_0 y\,.$$

Here, we have inserted the factor $\bar f(h_{sh}) = 1.19$ from Sec. IV B. The importance of using the correct demagnetization factor for the smaller spheres was established in the earlier experiments on β-Ga.[15] Equation (42)–(44) require an accurate knowledge of $H_c(t)$, which must be taken from the literature. We have used[24]

$$H_c(t) = H_0(1 - t^2)(1 - 0.11t^2)\,, \tag{47}$$

where $H_0 = 305.5$ Oe. This gives H_c accurate to 1 or 2%.

Figure 9 shows the superheating and supercooling results for the 15.4-μm sphere. The size effect in the coherence length close to T_c gives the customary increase in all κ's close to T_c. Neglecting this size effect, we see that κ_{sc} and $\kappa_{sh}^{\bar\delta}$ converge towards approximately the same values at $t = 1$, as they should. The extrapolated values in fact differ slightly, but a reduction of 1% in $H_c(T)$ would make them coincide, and this is less than the accuracy with which H_c is known.

To determine the GL parameter κ at $t = 1$, we use the parameter $\kappa_R^{\bar\delta}$, Eq. (45), which does not require knowledge of $H_c(t)$ nor a precise determination of T_c.[15] As shown in the upper part of Fig. 9, $\kappa_R^{\bar\delta}$ is extrapolated to $t = 1$ using the data $0.86 < t < 0.98$. The result for the GL parameter is

$$\kappa_{GL}(t = 1) = 0.093 \pm 0.001\,,$$

in excellent agreement with Feder and McLachlan's value[14] of 0.0926 ± 0.001, from their single-sphere experiments. It is also in fair agreement with the value of Smith *et al.* obtained on tin powders.[12] They found $\kappa_{Sn} = 0.087 \pm 0.002$, but they may have a

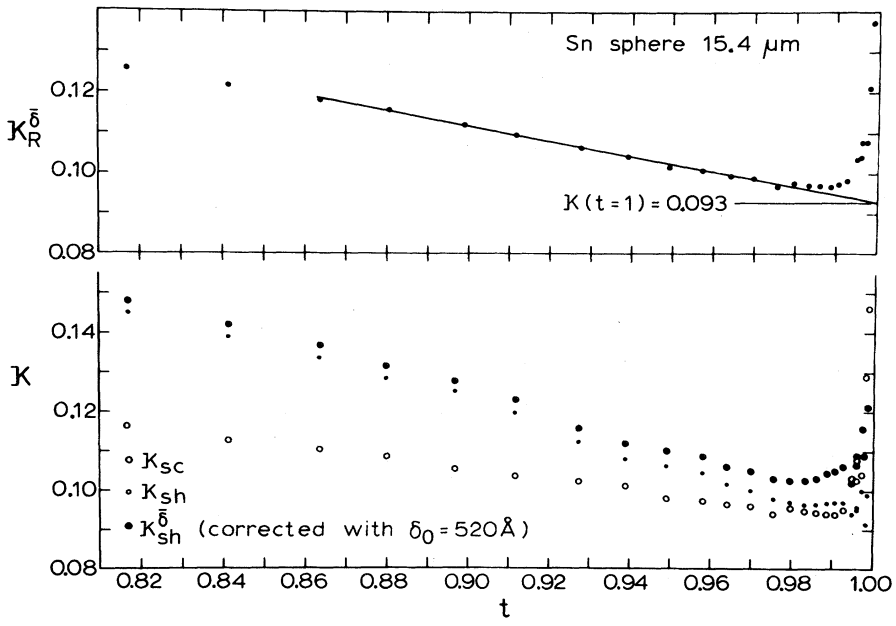

FIG. 9. Superheating and supercooling results for the 15.4-μm sphere. Different κ's are given by Eqs. (42)–(45). Ginzburg-Landau parameter at $t = 1$ is determined by extrapolation of $\kappa_R^{\bar\delta}$ (upper right). Notice onset of size effect at $t \approx 0.985$.

small systematic error due to the width of the supercooling transition in the powder experiments. Thus, within experimental error, all these measurements agree nicely as to the value of κ at $t=1$. Substituting our value of κ into Eq. (10) gives $H_{sh}^{bulk}=2.76H_c$ at $t=1$, which is the value used throughout the analysis of the field effect.

Finally, we give the (extrapolated) slopes of the different κ's at $t=1$. We find values of $(1/\kappa)(d\kappa/dt)_1$ of -1.5, -2.0, and -3.2 for κ_{sc}, $\kappa_R^{\bar{\delta}}$, and $\kappa_{sh}^{\bar{\delta}}$, respectively. The slope of κ_{sc} compares to a theoretical value of -1.0 for the GL parameter. Our value is identical to Feder and McLachlan's,[14] and is also in agreement with that obtained from the powder data of Smith *et al.* as inferred from Fig. 8 of Ref. 12.

V. DISCUSSION

The observation of a singularity in the field dependence of the penetration depth at H_{sh} provides yet another strong indication that we are indeed observing ideal superheating, i.e., the limit at which the normal phase is formed by homogeneous nucleation.

It is quite remarkable that both the temperature dependence (Fig. 3) and the field dependence (Figs. 4–6) of the penetration depth are unaffected by the onset of the size effect in the coherence length, which starts around $t=0.985$ for the 15.4-μm-diam sphere (Fig. 9). We have shown that even in this size-effect region, the field dependence is governed by H_{sh}^{bulk}, although the actual H_{sh} is reduced because of the size effect. However, this is not too surprising. The size effect in the coherence length becomes marked at $1-t\simeq 10^{-2}$. Since the penetration depth is roughly an order of magnitude smaller, and diverges as $1/(1-t)^{1/2}$ near T_c, a similar strong size effect in the penetration depth would not be expected to occur until $1-t\simeq 10^{-4}$, which is much closer to T_c than any of the present experiments.

Turning to the observed field dependence $f(H/H_c)$ of the penetration depth, Fig. 6, we can now invert Eqs. (5) and (6) to get a picture of the depression of the surface order parameter ψ_s as a function of the field H. This gives $\psi_s/\psi_0=f(h)^{-1}$ and $f(h)^{-3/2}$, respectively, for the local and nonlocal cases. Figure 10 shows the resulting curves for ψ_s/ψ_0 based on δ_{exp}, as well as the theoretical GL prediction, Eq. (11). The latter curve gives a value of 0.707 for ψ_s/ψ_0 at H_{sh}, while the experimental values are 0.663 and 0.540 using the local and nonlocal equations, respectively. Figure 10 thus indicates that the GL prediction, Eq. (11), is rather good, but that it may underestimate the depression of the order parameter at the superheating field. Although we do not know the exact relationship between $\delta(H)$ and $\psi_s(H)$, we can conclude on the basis of Fig. 10 that the surface order parameter ψ_s is depressed by (30–50)% at H_{sh}.

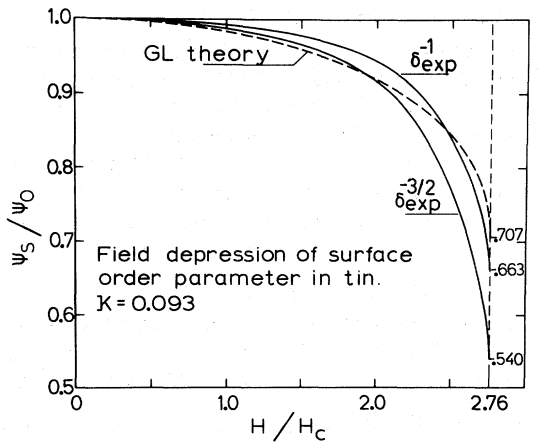

FIG. 10. Depression of the surface order parameter ψ_s as a function of the field H. Broken curve shows GL prediction [Eq. (11)]. Full curves are based on the experimental values of $\delta(H)$, with $\psi_s\sim\delta^{-1}$ and $\psi_s\sim\delta^{-3/2}$ for the local and nonlocal cases, respectively.

It would be of interest to determine how fast $f'(h)$ and $\psi_s'(h)$ diverge near H_{sh}, to look for deviations from mean-field theory, which predicts a divergence as $(1-H/H_{sh})^{-1/2}$. However, such an analysis is made complicated by the averaging over the spherical surface, and by the effect of the tickling field. The only conclusion that can be drawn is that the data seem to be consistent with a mean-field theory type of divergence near H_{sh}.

VI. CONCLUSION

In experiments on single tin spheres 15–30 μm in diameter, we have carried out the first measurements of the field dependence of the penetration depth up to the bulk superheating field, which is $2.76H_c$ for tin at $t=1$. In weak fields up to H_c, we find the customary weak quadratic field dependence. As the field increases towards the superheating limit, $\delta(H)$ increases greatly, reaching a value $\delta(H_{sh})/\delta(H=0)=1.51\pm0.04$. The experiments indicate that the first derivative of $\delta(H)$ diverges at H_{sh}, although this cannot be rigorously proven. The analysis indicates that the depression in the surface order parameter ψ_s is (30–50)% at H_{sh}. Experiments are in progress to extend the measurements to different materials with a different κ.

ACKNOWLEDGMENTS

I wish to thank T. Ottinsen for his continuous help and interest in the analysis of the experimental data. I am grateful to Professor A. B. Pippard for some fruitful comments, and to Professor J. Feder for helpful discussions.

---

*Work partially supported by a grant from the Norwegian Research Council for Science and the Humanities (NAVF).

[1]D. Shoenberg, Proc. R. Soc. A 175, 49 (1940).
[2]M. Désirant and D. Shoenberg, Proc. Phys. Soc. Lond. 60, 413 (1948).
[3]E. Laurmann and D. Shoenberg, Proc. R. Soc. A 198, 560 (1949).
[4]A. Schawlow and G. Devlin, Phys. Rev. 113, 120 (1959).
[5]P. Dheer, Proc. R. Soc. A 260, 333 (1961).
[6]B. Maxfield and W. McLean, Phys. Rev. 139, A1515 (1965).
[7]A. B. Pippard, Proc. R. Soc. A 203, 210 (1950).
[8]Y. V. Sharvin and V. F. Gantmakher, Zh. Eksp. Teor. Fiz. 39, 1242 (1960) [Sov. Phys.-JETP 12, 866 (1961)].
[9]F. Behroozi, M. P. Garfunkel, F. H. Rogan, and G. A. Wilkinson, Phys. Rev. B 10, 2756 (1974).
[10]V. L. Ginzburg and L. D. Landau, Zh. Eksp. Teor. Fiz. 20, 1064 (1950).
[11]J. Feder, S. R. Kiser, and F. Rothwarf, Phys. Rev. Lett. 17, 87 (1966).
[12]F. W. Smith, A. Baratoff, and M. Cardona, Phys. Kondens. Mater. 12, 145 (1970).
[13]F. de la Cruz, M. D. Maloney, and M. Cardona, Phys. Rev. B 3, 3802 (1971).
[14]J. Feder and D. S. McLachlan, Phys. Rev. 177, 763 (1969).
[15]H. Parr and J. Feder, Phys. Rev. B 7, 166 (1973).
[16]A. B. Pippard, Proc. R. Soc. A 216, 547 (1953).
[17]See, for example, *Superconductivity*, edited by R. D. Parks (Dekker, New York, 1969), Vol. I, pp. 90–93 and 171–179.
[18]V. L. Ginzburg, Zh. Eksp. Teor. Fiz. 34, 113 (1958) [Sov. Phys.-JETP 7, 78 (1958)].
[19]*Quantum Fluids*, edited by D. F. Brewer (North-Holland, Amsterdam, 1966), p. 26.
[20]F. London, *Superfluids* (Wiley, New York, 1950), p. 35.
[21]Tin of nominal purity 99.999% from Koch-Light Laboratories.
[22]H. Parr, Phys. Rev. B 10, 4572 (1974).
[23]P. M. Tedrow, G. Faraci and R. Meservey, Phys. Rev. B 4, 74 (1971).
[24]For temperatures $t^2 > 0.6$, this gives a good fit to the data of D. K. Finnemore and D. E. Mapother, Phys. Rev. 140, A 507 (1965); R. W. Shaw, D. E. Mapother, and D. C. Hopkins, *ibid.* 120, 88 (1960).